

## Elastic positron-cadmium scattering at low energies

M. W. J. Bromley\*

*Department of Physics and Computational Science Research Center, San Diego State University, San Diego, California 92182, USA*

J. Mitroy†

*ARC Centre for Antimatter-Matter Studies and School of Engineering, Charles Darwin University, Darwin, Northern Territory 0909, Australia*

(Received 13 March 2010; published 25 May 2010)

The elastic and annihilation cross sections for positron-cadmium scattering are reported up to the positronium-formation threshold (at 2.2 eV). The low-energy phase shifts for the elastic scattering of positrons from cadmium were derived from the bound and pseudostate energies of a very large basis configuration-interaction calculation of the  $e^+$ -Cd system. The  $s$ -wave binding energy is estimated to be  $126 \pm 42$  meV, with a scattering length of  $A_{\text{scat}} = (14.2 \pm 2.1)a_0$ , while the threshold annihilation parameter,  $Z_{\text{eff}}$ , was  $93.9 \pm 26.5$ . The  $p$ -wave phase shift exhibits a weak shape resonance that results in a peak  $Z_{\text{eff}}$  of  $91 \pm 17$  at a collision energy of about  $490 \pm 50$  meV.

DOI: [10.1103/PhysRevA.81.052708](https://doi.org/10.1103/PhysRevA.81.052708)

PACS number(s): 34.80.Uv, 34.80.Bm, 31.15.A–, 03.65.Nk

Calculations over the past decade have demonstrated that positrons can form bound states with a wide range of neutral atoms [1,2]. Apart from the intrinsic interest in the quantum mechanics of these systems, the strong evidence for positron binding to atoms has provided support for the hypothesis that positron-molecule bound states associated with vibrationally excited states are predominantly responsible for the massive positron annihilation rates observed in many molecular-gas experiments [3]. The experimental realization and identification of positronic atoms and molecules is very difficult, so evidence for their existence is best sought indirectly by means of scattering experiments.

The first-principles calculation of positron-atom interactions is a challenging proposition due to the tendency for the atomic electrons to localize around the positron, forming a composite structure somewhat akin to the positronium (Ps) atom [1,4]. The configuration-interaction (CI) method has been used to determine the energies of the positronic magnesium ( $e^+$ -Mg) and positronic zinc ( $e^+$ -Zn) ground states. In addition, their low-energy elastic and annihilation cross sections have been extracted from the energies of physical and low-energy pseudostates [5,6]. The presence of a Ps-like cluster dramatically slows down the convergence of the CI expansion with respect to the partial waves included in the orbital basis [1,4]. For example, the prediction of the  $^2P^o$  excited state of  $e^+$ -Ca was performed with a CI basis of dimension 900 000 [7,8]. Even then, the prediction of binding was reliant on an extrapolation to the  $\ell \rightarrow \infty$  limit.

The recent calculation upon the positron-magnesium system ( $e^+$ -Mg), which supports an electronically stable  $^2S^e$  bound state, revealed the presence of a prominent  $p$ -wave-shape resonance at 0.096 eV incident energy [5,6]. This represented the first solid evidence that the positron-atom interaction could lead to the formation of shape resonances. Experimental searches for shape resonances in other atoms with monochromatic (sub-50-meV) positron beams have not yet been successful [9], despite the rich resonance

structures that are present in electron-atom scattering experiments [10]. Other calculations on the positron-copper and positron-zinc systems (which both support a  $^2S^e$  bound state) revealed a structure in their low-energy annihilation spectrum due to a weak resonance in their  $^2P^o$  scattering channels [6,11].

The reason for the strong structure in the  $e^+$ -Mg system, and the weaker structures in the  $e^+$ -Cu and  $e^+$ -Zn systems, is the attractive polarization interaction between the atom and the positron. The magnesium atom has a dipole polarizability,  $\alpha_d$ , of 71.35 a.u. [12–15] (an atomic unit corresponds to one  $a_0^3$ ), while that of copper is  $41.7 \pm 3.4$  a.u. [16] (there are other estimates that lie toward the upper side of this [15]) and that of zinc is  $38.8 \pm 0.8$  a.u. [17]. The cadmium atom is a good candidate to support a  $^2P^o$  shape resonance since it has a dipole polarizability between 44 and 50 a.u. [15,18–20] and is also known to bind a positron [21,22].

The present paper reports on improved CI calculations of the  $e^+$ -Cd bound state and the  $e^+$ -Cd elastic scattering and annihilation cross sections. The orbital basis sets are larger, and thus estimates of the elastic and annihilation cross sections are better than previous work [22]. The CI energies of the bound and positive-energy pseudostates were used to determine an effective positron-cadmium interaction and thus estimate the cross section for elastic scattering below 2.2 eV. This effective interaction is better characterized than that used in Ref. [22] since four energies were used in its construction. This approach has been validated on the  $e^+$ -H and  $e^+$ -Cu scattering systems and was previously used to determine the low-energy  $e^+$ -Mg and  $e^+$ -Zn elastic and annihilation cross sections [5,6]. It is shown here that cadmium possesses a weak  $p$ -wave-shape resonance, as seen in the elastic (total) scattering cross section and more visibly in the low-energy dependence of the annihilation parameter,  $Z_{\text{eff}}(k)$ .

There have been a number of theoretical analyses of the positron-cadmium system by other groups. Optical potential calculations neglecting Ps formation have been reported at energies from 40 to 150 eV [23] and from 6.4 to 300 eV [24]. A relativistic polarized orbital calculation [25] also reported cross sections for positron-cadmium scattering. This calculation, despite only allowing for dipole excitation, suggested

\*mbromley@physics.sdsu.edu

†jim.mitroy@edu.edu.au

that the positron could be bound to cadmium with a binding energy of 0.000 056 hartree. Another prediction of positron binding had been obtained with many-body perturbation theory (MBPT) [26]. The MBPT calculation had a binding energy of 0.0129 hartree [26], which is significantly larger than an explicit CI calculation, which gave a binding energy of  $\approx 0.0061$  hartree [21,22]. The MBPT calculation is believed to significantly overestimate the strength of the positron-atom interaction [1].

## I. STRUCTURE AND PROPERTIES OF NEUTRAL CADMIUM

The semiempirical Hamiltonian used in the present large-scale CI calculations is identical to that used previously for  $e^+Cd$  [22]. In brief, the model Hamiltonian for the  $Cd^{2+}$  core is initially based on a Hartree-Fock (HF) wave function for the neutral Cd ground state. One- and two-body semiempirical polarization potentials are then added whose cutoff parameters are tuned to reproduce the  $Cd^+$  atomic spectrum using statistical averaging of the fine-structure doublets. The effective Hamiltonian for a system with two valence electrons would be written as

$$H = \sum_{i=1}^2 \left[ -\frac{1}{2} \nabla_i^2 + V_{\text{dir}}(\mathbf{r}_i) + V_{\text{exc}}(\mathbf{r}_i) + V_{\text{p1}}(\mathbf{r}_i) \right] + \frac{1}{r_{12}} + V_{\text{p2}}(\mathbf{r}_1, \mathbf{r}_2). \quad (1)$$

The  $V_{\text{dir}}$  and  $V_{\text{exc}}$  potentials represent the direct and exchange interactions with the core electrons. They are computed without approximation using core wave functions calculated with the HF method [13,27]. The one-body polarization interaction  $V_{\text{p1}}(r)$  is semiempirical in nature and can be written in its most general form as an  $\ell$ -dependent potential, that is,

$$V_{\text{p1}}(\mathbf{r}) = - \sum_{\ell m} \frac{\alpha_{\text{core}} g_{\ell}^2(r)}{2r^4} |\ell m\rangle \langle \ell m|. \quad (2)$$

The coefficient,  $\alpha_{\text{core}} = 4.971$  a.u. [28], is the static dipole polarizability of the  $Cd^{2+}$  core, and  $g_{\ell}^2(r) = [1 - \exp(-r^6/\rho_{\ell}^6)]$

is a cutoff function that eliminates the  $1/r^4$  singularity at the origin. The cutoff parameters,  $\rho_{\ell}$ , were tuned to reproduce the binding energies of the  $Cd^+$  single-electron valence states. The two-electron, or dielectronic, polarization potential is written as

$$V_{\text{p2}}(\mathbf{r}_i, \mathbf{r}_j) = - \frac{\alpha_{\text{core}}}{r_i^3 r_j^3} (\mathbf{r}_i \cdot \mathbf{r}_j) g(r_i) g(r_j). \quad (3)$$

The two-body cutoff parameter,  $g(r)$ , was chosen to be the average of the  $\rho_{\ell}$ 's, which are given in Ref. [22].

While the Hamiltonian is the same as that used in Ref. [22], the single-electron basis is significantly larger. The number of single-electron orbitals per partial wave used here are  $N_{\ell=0..4} = 19, 18, 18, 16, 16$ . This generates nearly double the number of two-electron configurations compared to that used previously [22]. The properties of the present two-electron model of Cd were close to converging. An earlier calculation including orbitals with  $\ell = 10$  revealed a 0.02-a.u. change in the dipole polarizability when  $\ell$  was increased from 3 to 10 [22]. Table I provides a summary of some relevant properties of the cadmium ground state including the dipole polarizability.

There is some uncertainty about the dipole polarizability of neutral Cd. The present calculation gives 50.03 a.u., while one experiment gave  $49.6 \pm 1.6$  a.u. [18]. However, another measurement by the same group gave  $45.3 \pm 0.2$  a.u. [19]. A relativistic calculation using a core potential and semiempirical polarization potential similar in style to the present work gave 44.63 a.u. [20]. These smaller estimates of the Cd polarizability are to be preferred for reasons outlined previously [22].

The present semiempirical method has been shown to describe the long-range properties of many atoms such as Mg and Ca to an accuracy of a couple of percentage points [13]. However, there appears to be some degradation in accuracy for the Cd system. The most important parameter is the polarizability, and the present calculation appears to overestimate this by about 10%. The present model of the Cd atom is adequate to describe positron scattering, and some discussion of the uncertainty that arises from an imperfect model is presented later.

TABLE I. Calculations of the atomic structure of neutral Cd with the maximum angular momentum of the orbitals included ( $L_{\text{int}}$ ). The number of configurations is given in the  $N_{\text{CI}}$  column. The  $E$  column is the  $^1S^e$  ground-state energy relative to the energy of the  $Cd^{2+}$  core (energies are given in hartrees). For the primary  $^1S^e$  to  $^1P^o$  transition,  $\Delta E$  is the energy difference, while  $f_{if}$  is the oscillator strength. The dipole polarizability,  $\alpha_d$ , is given in atomic units and includes a contribution from the core. For comparison, the rows marked with an asterisk (\*) correspond to two results:  $L_{\text{int}} = 3$  and 10 from Ref. [22]. The experimental results for the energies, oscillator strengths, and polarizabilities are taken from various sources [18,19,29–31] and, where available, their uncertainties in the last digits are given in parentheses.

$L_{\text{int}}$	$N_{\text{CI}}$	$E$	$\Delta E$	$f_{if}$	$\alpha_d$
3	668	−0.939 3428	0.186 7173	1.5141	49.934
4	804	−0.939 5156	0.186 4624	1.5143	50.027
3*	361	−0.939 1903	0.186 2284	1.511	50.07
10*	613	−0.939 4978	0.186 2830	1.513	50.09
Theory [20]					44.63
Exp. [18,29–31]		−0.951 880	0.199 078	1.30(10)	49.6(16)
Exp. [19]					45.31(20)

## II. CONFIGURATION INTERACTION CALCULATIONS OF $e^+Cd$

The  $e^+Cd$  CI wave function consists of a linear combination of three-particle states which are antisymmetric in the interchange of the two electrons,

$$|\Psi; L_T S_T\rangle_a = \sum_i c_i |\Phi_i; L_T S_T\rangle_a. \quad (4)$$

Each antisymmetrized state is constructed as a linear combination of coupled but not antisymmetrized states. Two electrons (particles 1 and 2) are coupled first to each other, and then the positron (particle 0) is coupled to form a state with net angular and spin angular momenta,  $L_T$  and  $S_T$ . The antisymmetric states are written as

$$|\Phi_i; [ab]L_I S_I p L_T S_T\rangle_a = N_{ab}(|[a_1 b_2]L_I S_I p_0\rangle + (-1)^\Pi |[b_1 a_2]L_I S_I p_0\rangle), \quad (5)$$

where the subscript by each orbital denotes the electron occupying that particular orbital,  $N_{ab} = 1/\sqrt{2(1 + \delta_{ab})}$  and  $\Pi = \ell_a + \ell_b + L_I + S_I$ .

The CI basis was constructed by letting the two electrons and the positron form all the possible configuration with a total angular momentum of  $L_T$ , with the two electrons in a spin-singlet state, subject to the selection rules,

$$\max(\ell_0, \ell_1, \ell_2) \leq L_{\max}, \quad (6)$$

$$\min(\ell_1, \ell_2) \leq L_{\text{int}}, \quad (7)$$

$$(-1)^{(\ell_0 + \ell_1 + \ell_2)} \equiv +1 \text{ or } -1. \quad (8)$$

Here,  $\ell_0$ ,  $\ell_1$ , and  $\ell_2$  are respectively the orbital angular momenta of the positron and the two electrons. The even [odd] parity states require  $(-1)^{(\ell_0 + \ell_1 + \ell_2)} \equiv +1$  [ $-1$ ].

The Hamiltonian for the  $e^+Cd$   $2S^e$  state was diagonalized in a CI basis including orbitals up to  $L_{\max} = 12$ . There were a minimum of sixteen radial basis functions for each  $\ell$ . There were nineteen  $\ell = 0$  positron orbitals. The largest  $2S^e$  calculation was performed with  $L_{\max} = 12$  and  $L_{\text{int}} = 4$ . The  $L_{\text{int}}$

parameter does not have to be large since it is mainly concerned with describing the more quickly converging electron-electron correlations [12]. The CI basis for the  $2P^o$  symmetry included a minimum of sixteen radial basis functions for each  $\ell$ . There were twenty  $\ell = 1$  positron orbitals. The largest  $2P^o$  calculation was performed with  $L_{\max} = 10$  and  $L_{\text{int}} = 3$ . The overall dimensionalities in the  $2S^e$  calculation are about an order of magnitude larger than the previous calculation [22] but were severely impeded by anomalously slow convergence of the (iterative) Davidson diagonalization algorithm [32].

One difficulty present in all CI calculations of positron-atom interactions is the slow convergence of the energy with  $L_{\max}$  [1,33,34]. It is necessary to perform a series of calculations with successively larger values of the maximum  $\ell$  of the single-particle orbitals in order to extrapolate to the  $L_{\max} \rightarrow \infty$  limit. Justification of the procedure to handle this problem can be found elsewhere [34–37]. The present calculation is reliant on an asymptotic analysis that utilizes the result that successive increments,  $\Delta E_L = \langle E \rangle_L - \langle E \rangle_{L-1}$ , and can be written as an inverse power series [35,36], viz.

$$\Delta E_L \approx \frac{A_E}{(L + \frac{1}{2})^4} + \frac{B_E}{(L + \frac{1}{2})^5} + \frac{C_E}{(L + \frac{1}{2})^6} + \dots \quad (9)$$

The  $L_{\max} \rightarrow \infty$  limits have been determined by fitting sets of  $\langle E \rangle_L$  values to an asymptotic series with one, two, or three terms. The factors  $A_E$ ,  $B_E$ , and  $C_E$  for the three-term expansion are determined at a particular  $L_{\max}$  from four successive energies ( $\langle E \rangle_{L-3}$ ,  $\langle E \rangle_{L-2}$ ,  $\langle E \rangle_{L-1}$ , and  $\langle E \rangle_L$ ). The series is summed to  $\infty$  once the linear factors have been determined. Calculations of the annihilation rate are handled in a similar way, but the leading power in the inverse power series is two. The efficacy of these procedures in handling positronic problems has been demonstrated elsewhere [34].

A summary of  $e^+Cd$  expectation values taken to the  $L_{\max} \rightarrow \infty$  limit are given in Table II. The binding energy  $\varepsilon$  for each symmetry is calculated with respect to the energy of the Cd ground state using the basis for that symmetry. The

TABLE II. Results of CI calculations for  $e^+Cd$  with total orbital angular momentum  $L_T = 0$  and  $L_T = 1$  vs  $L_{\max}$ . The two lowest eigenstates computed in each symmetry are given (denoted by  $M$ ). The total number of electron and positron orbitals, and resulting configurations, are denoted by  $N_e$ ,  $N_p$ , and  $N_{\text{CI}}$ . The three-body energy (in hartrees) of the  $e^+Cd$  system, relative to the energy of the  $Cd^{2+}$  core, is denoted by  $\langle E \rangle_{L_{\max}}$ , while  $\varepsilon = |E(e^+Cd)| - |E(Cd)|$  gives the binding energy against dissociation into  $e^+Cd$ . Both  $\langle r_e \rangle$  and  $\langle r_p \rangle$ , are given in  $a_0$ . The valence  $\Gamma_v$  and core  $\Gamma_c$  annihilation rates are given in units of  $10^9 \text{ sec}^{-1}$ . The results in the  $\infty$  rows are from various  $L_{\max} \rightarrow \infty$  extrapolations as discussed in the text. The results in the row labeled with an asterisk (\*) are taken from an earlier calculation [22].

$L_T$	$M$	$L_{\max}$	$N_e$	$N_p$	$N_{\text{CI}}$	$\langle E \rangle_{L_{\max}}$	$\langle \varepsilon \rangle_{L_{\max}}$	$\langle r_e \rangle_{L_{\max}}$	$\langle r_p \rangle_{L_{\max}}$	$\langle r_{ep}^2 \rangle_{L_{\max}}$	$\langle \Gamma_c \rangle_{L_{\max}}$	$\langle \Gamma_v \rangle_{L_{\max}}$
0	1	9	167	160	398 864	-0.944 508 209	0.004 992 569	3.099 718	9.175 120	113.621	0.035 097	0.289 868
0	1	10	183	176	463 632	-0.944 738 485	0.005 222 845	3.104 804	9.070 876	110.498	0.035 663	0.310 873
0	1	11	199	192	528 400	-0.944 914 359	0.005 398 719	3.109 054	8.983 412	108.020	0.036 149	0.329 395
0	1	12	215	208	593 168	-0.945 050 398	0.005 534 757	3.112 366	8.923 587	106.298	0.036 478	0.344 965
0	1	$\infty$				-0.945 688 025	0.006 172 384	3.131 605	8.741 339	100.722	0.037 458	0.524 294
0*	1	$\infty$				-0.945 291	0.006 100	3.1284	8.7819	-	0.037 73	0.5273
0	2	12	215	208	593 168	-0.937 163 752	-0.002 351 889	2.991 739	33.536 157	1231.460	0.003 169	0.026 248
0	2	$\infty$				-0.937 177 494	-0.002 338 147	-	-	-	-	-
1	1	10	183	180	901 816	-0.932 692 278	-0.006 650 529	3.000 202	19.747 390	438.675	0.001 215	0.015 984
1	1	$\infty$				-0.932 790 051	-0.006 552 756	3.002 587	19.293 332	412.082	0.001 254	0.031 316
1	2	10	183	180	901 816	-0.921 287 707	-0.018 055 100	3.057 062	16.904 543	379.403	0.006 010	0.091 969
1	2	$\infty$				-0.921 814 129	-0.017 528 678	-	-	-	-	-

overall binding energy of the  $^2S^e$  ground state was 0.006 172 hartree, while the first pseudostate was located at an energy of 0.002 532 hartree above the elastic scattering threshold. The energies of the two lowest pseudostates of  $^2P^o$  symmetry were 0.003 989 and 0.012 012 hartree above threshold, respectively.

Extrapolated expectation values are not given for some of the operators in Table II. The extrapolation was unreliable for these specific state-operator combinations.

### III. GENERATING PHASE SHIFTS FROM THE PSEUDOSTATE METHOD

#### A. The effective potential

The scattering phase shifts were derived from the energies in Table II by constructing an effective operator that gave exactly the same binding energies and then using that operator to compute the phase shifts. This effective potential of the target can be written formally as

$$V_{\text{opt}}(r) = V_{\text{dir}}(r) + V_{\text{pol}}(r). \quad (10)$$

The potential  $V_{\text{dir}}$  is the direct interaction between the target and projectile. This can be approximated by the direct interaction between the projectile and the target HF ground-state wave function,  $\Omega_{\text{HF}}$ , which can have a slightly different density from the CI ground state,  $\Omega_{\text{gs}}$  [6].

The polarization potential  $V_{\text{pol}}(r)$  is semiempirical in nature, with the form [5,22,38,39]

$$V_{\text{pol}}(r) = -\frac{\alpha_d g_d^2(r)}{2r^4} - \frac{A_Q g_Q^2(r)}{2r^6}. \quad (11)$$

The  $\alpha_d$  is the static dipole polarizability of the neutral atomic target [5,22,38,39]. The cutoff functions are defined as  $g_d^2 = [1 - \exp(-r^6/\rho^6)]$  while  $g_Q^2 = [1 - \exp(-r^8/\rho^8)]$ . The second term has a functional form similar to that expected for a quadrupole polarization; however, the  $A_Q$  parameter was treated as an adjustable parameter. The actual parameters of the specific potentials used for  $L_T = 0$  and  $L_T = 1$  are listed in Table III. These parameters were fixed to the two lowest energy states for  $L_T = 0$  and  $L_T = 1$ .

#### B. Phase shifts and elastic scattering

The low-energy  $s$ -wave phase shifts were computed with the effective  $s$ -wave potential as given in Table III. The phase

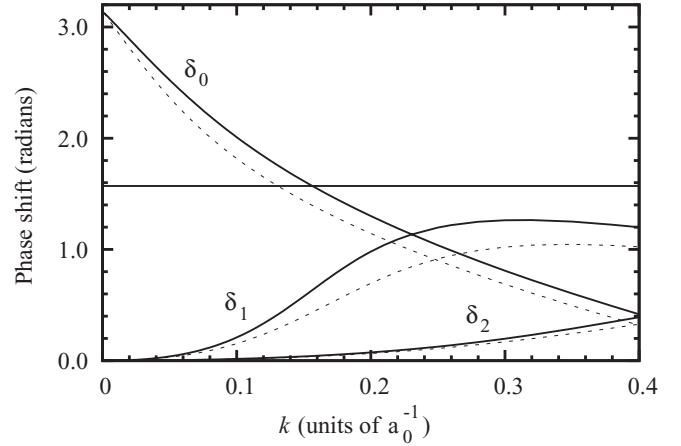


FIG. 1. The  $s$ -,  $p$ -, and  $d$ -wave phase shifts for elastic scattering of positrons from cadmium in the energy region below the Ps-formation threshold at  $k \approx 0.4a_0^{-1}$ . The dashed curves were all computed with a weaker polarization potential to estimate the uncertainty in the phase shifts.

shifts for  $L_T \geq 1$  were all computed with the  $p$ -wave potential. The phase shifts are plotted in Fig. 1. The  $L_T = 0$  and  $L_T = 1$  phase shifts are in opposite quadrants for  $k < 0.156a_0^{-1}$ . One consequence of this is that the differential cross section will be larger at backward angles than at forward angles from threshold to  $k = 0.156a_0^{-1}$  [22]. A measurement of the differential cross section in this energy region would provide strong circumstantial evidence that positrons can form bound states with the cadmium atom.

The  $L_T = 1$  phase shift increases quickly until  $k \approx 0.3a_0^{-1}$ . This structure can be regarded as a weak shape resonance caused by the strong polarization potential between the positron and the atom. The main difference from earlier work [22] lies in the  $L_T = 1$  phase shift. The present phase shift achieves a peak value of 1.260 rad at  $k = 0.31a_0^{-1}$ . The earlier model potential calculation gave a maximum phase shift of 0.89 rad at  $k \approx 0.40a_0^{-1}$  [22].

The elastic scattering cross section shown in Fig. 2 shows evidence of the strongly rising  $p$ -wave phase shift in the form of a plateau at  $k \approx 0.15a_0^{-1}$ . The scattering length of  $12.1a_0$  results in a large threshold cross section of  $1840a_0^2$ . The present scattering length is 4% larger than the previous estimate based

TABLE III. Parameter definitions of the  $V_{\text{pol}}$  effective polarization potentials used to describe  $s$ -wave and  $p$ -wave scattering for the  $e^+$ -Cd system [as per Eq. (11)]. The  $s$ -wave potentials were tuned to the properties of the  $^2S^e$  ground state and the lowest energy pseudostate, while the  $p$ -wave potentials were tuned to the two lowest energy  $p$ -wave pseudostates. The annihilation enhancement parameters that were used are given in the  $G_c$  and  $G_v$  columns. The binding energy  $\varepsilon$  (in hartrees) is positive for bound states and negative for pseudostates. The mean positron radius and scattering length,  $A_{\text{scat}}$ , are in units of  $a_0$ . The core and valence annihilation rates for the lowest energy state are given in units of  $10^9 \text{ s}^{-1}$ . The rows denoted by the asterisks (\*) correspond to calculations with weakened polarization potentials to estimate the uncertainty in the calculations.

$L$	$\alpha_d$	$A_Q$	$\rho$	$G_c$	$G_v$	$\varepsilon$	$\langle r_p \rangle$	$\langle \Gamma_c \rangle$	$\langle \Gamma_v \rangle$	$A_{\text{scat}}$
0	50.1	900.0	3.936	2.5	17.3	0.006 163	8.70	0.007 38	0.5273	12.1
0*	45.1	810.0	3.936	2.5	17.3	0.003 133	10.70	0.005 33	0.3676	16.3
1	50.1	500.0	3.349	2.5	17.0	-0.006 560	19.5	0.004 54	0.031 32	-
1*	45.1	450.0	3.349	2.5	17.0	-0.006 809	20.1	0.002 96	0.018 16	-

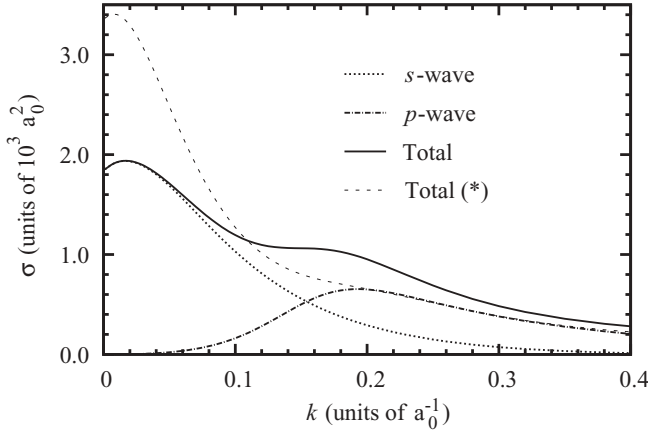


FIG. 2. The elastic scattering cross section for  $e^+$ -Cd scattering as a function of  $k$  (in units of  $a_0^{-1}$ ) as calculated with the  $V_{\text{pol}}$  potential in the energy region below the Ps-formation threshold at  $k \approx 0.4a_0^{-1}$ . The solid line shows the total cross section while the dotted and dot-dashed curves show the  $L_T = 0$  and  $L_T = 1$  partial cross sections. The dashed curve (denoted by the asterisk) is the elastic scattering cross section as computed with a weaker polarization potential to estimate the uncertainty in the cross section.

on a smaller CI wave function and a one-parameter polarization potential [22].

### C. Positron annihilation

Besides obtaining the phase shifts in the low-energy region, it is also possible to determine the annihilation parameter,  $Z_{\text{eff}}$  [40–42]. The fundamental idea is to compare exact and model potential calculations of  $Z_{\text{eff}}$  and so fix the enhancement factor,  $G$  [39,43,44]. Enhancement factors were first introduced in the calculation of the annihilation rate of positrons in condensed matter systems [45–47]. They incorporate the tendency for attractive electron-positron correlations to increase the electron density in the immediate vicinity of the positron.

It has been shown that model potential calculations of  $s$ -wave positron scattering from hydrogen and helium that were tuned to give the correct phase shift at a reference energy also reproduced the low-energy behavior of  $Z_{\text{eff}}(k)$  up to a multiplying constant (i.e.,  $G$ ) [39]. The annihilation parameter for the model potential wave function follows the model of Mitroy and Ivanov [39] and is written as

$$Z_{\text{eff}} = \int d^3r [G_v \rho_v(\mathbf{r}) + G_c \rho_c(\mathbf{r})] |\Phi_{\text{opt}}(\mathbf{r})|^2, \quad (12)$$

where  $\rho_c(\mathbf{r})$  and  $\rho_v(\mathbf{r})$  are the electron densities associated with the core and valence electrons of the target atom and  $\Phi_{\text{opt}}(\mathbf{r})$  is the positron scattering function obtained in the tuned model potential.

For the core orbitals,  $G_c$  is set to 2.5 due to reasons outlined in Ref. [39]. The valence enhancement factor  $G_v$  is computed by the simple ratio

$$G_v = \frac{\Gamma_v^{CI}}{\Gamma_v^{\text{model}}}, \quad (13)$$

where  $\Gamma_v^{CI}$  is the annihilation rate of the positron with the valence orbitals as given by the CI calculation and  $\Gamma_v^{\text{model}}$  is

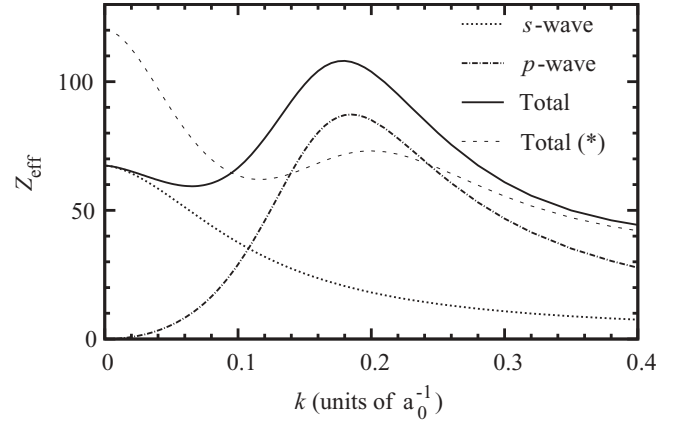


FIG. 3. The annihilation parameter,  $Z_{\text{eff}}$ , for  $e^+$ -Cd scattering as a function of  $k$  (in units of  $a_0^{-1}$ ) as calculated with the  $V_{\text{pol}}$  potential in the energy region below the Ps-formation threshold at  $k \approx 0.4a_0^{-1}$ . The dotted and dot-dashed curves show the  $L_T = 0$  and  $L_T = 1$  partial contributions to  $Z_{\text{eff}}$  (the solid line). The dashed curve (denoted by the asterisk) is the  $Z_{\text{eff}}$  as computed with a weaker polarization potential to estimate the uncertainty in  $Z_{\text{eff}}$ .

the valence annihilation rate predicted by the model potential calculation with  $G = 1$ . The values adopted here are shown in Table III. This procedure reproduces the  $Z_{\text{eff}}(k)$  dependence in  $e^+$ -Cu scattering as explicitly computed by the CI-Kohn variational scattering method [6].

Figure 3 shows the annihilation parameter for  $k \leq 0.4a_0^{-1}$ . The threshold value of  $Z_{\text{eff}}$  was 67.4, about 15% smaller than a previous estimate of 80.1 [22]. The most notable feature is the peak in  $Z_{\text{eff}}$  at  $k \approx 0.18a_0^{-1}$ . This peak is a consequence of the structure in the  $p$ -wave phase shift. The value of  $Z_{\text{eff}}$  at the maximum was 108. The previous calculation only exhibited a weak peak of 46.3 at  $k \approx 0.2a_0^{-1}$  [22].

### D. Uncertainties

As discussed in a previous work [22], it is likely that the present model of Cd overestimates the neutral Cd polarizability. The calculations of Ye and Wang [20] gave a polarizability of 44.63 a.u. An estimate has been made of the tendency for the present CI calculation to overestimate the binding energy by repeating the effective potential calculations with slightly different potentials. To do this, the values of  $\alpha_d$  and  $A_Q$  in Table III were reduced by 10%, and the calculations of the phase shifts, cross section, and annihilation parameter were repeated. The values of  $\rho$  and  $G_v$  were not changed.

When this was done, the  $e^+$ Cd binding energy decreased from 0.0062 to 0.0031 hartree while the scattering length increased to  $16.3a_0$ . The binding energy of 0.0031 hartree is smaller than the  $e^+$ Zn binding energy of 0.0037 hartree [6]. Since Zn has an  $\alpha_d = 38.8 \pm 0.8$  a.u. [17], which is 20% lower than the present Cd model, this indicates that the  $\alpha_d = 45.1$  a.u. calculation underestimates the strength of the polarization potential.

The change in the phase shifts from the use of the alternate optical potential is depicted as the dashed curves in Fig. 1. In particular, the structure in the  $p$ -wave phase shift is less pronounced, and the maximum value achieved was 1.05 rad at  $k = 0.35a_0^{-1}$ .

The impact on the cross section and  $Z_{\text{eff}}$  are depicted as the dashed curves in Figs. 2 and 3. Only the total elastic cross section and the total  $Z_{\text{eff}}$  are shown. The zero-energy cross section is larger, while the shoulder in the elastic cross section is no longer obvious. The peak in  $Z_{\text{eff}}$  is still present but is not as prominent, and it has moved to a higher energy.

The present best estimates are taken to be midway between the results of the actual and the 10% reduced polarization potentials. The calculations with a polarizability of 50.1 a.u. overestimate the strength of the polarization interaction. The model potential calculations with a polarizability of 45.1 a.u. underestimate the strength of the attractive polarization potential. The best estimates are simply chosen to lie midway between these upper and lower bounds, as no additional constraints are currently available that would skew the best estimate in one direction or the other.

The  $e^+\text{Cd}$  binding energy should thus be taken to be  $\varepsilon = 0.46 \pm 0.15$  hartree ( $126 \pm 42$  meV) with a scattering length of  $A_{\text{scat}} = 14.2 \pm 2.1a_0$ . At threshold, the elastic scattering cross section  $\sigma = 2595 \pm 755a_0^2$  while  $Z_{\text{eff}} = 93.9 \pm 26.5$ . The weak  $p$ -wave-shape resonance manifests, at a collision energy of  $0.49 \pm 0.05$  eV, a peak  $Z_{\text{eff}} = 91 \pm 17$ .

#### IV. CONCLUSION

The CI method using a semiempirical *core* potential for the core-valence interactions [48] is applied to compute the energy and structure of the lowest two  $e^+\text{Cd}$  eigenstates in both the  $^2S^e$  and  $^2P^o$  symmetries. The close-to-threshold phase shifts are then extracted using the energies of the bound states or the positive energy pseudostates to tune an *optical* potential. The present estimates of the cross section are an improvement on previous work [22]. Using additional pseudostate energies to define the optical potential resulted in more reliable phase shifts and cross sections.

Structures related to a weak  $p$ -wave-shape resonance exist in both the elastic cross section and  $Z_{\text{eff}}$ . There is a shoulder in

the elastic cross section at an energy of about  $0.41 \pm 0.11$  eV. The annihilation parameter has a local peak of  $91 \pm 17$  at an energy of  $0.49 \pm 0.05$  eV. These results are a major departure from the behavior of a previous calculation of low-energy  $e^+\text{-Cd}$  scattering [22], where no such structure was observed. A graphical comparison of the (strong)  $V_{\text{pol}}$  calculation against those of  $e^+\text{-Mg}$ ,  $e^+\text{-Cu}$ , and  $e^+\text{-Zn}$  was recently published [2], clearly showing that  $e^+\text{-Mg}$  exhibits the strongest known resonance.

The present results also show that the  $e^+\text{Cd}$   $p$ -wave cross section stays below  $\pi/2$  for  $k < 0.143 \pm 0.013a_0^{-1}$  ( $E < 289 \pm 59$  meV). At these energies, there is a backward-peaked differential cross section whose measurement would give strong, albeit indirect, evidence of positron binding to cadmium. The present results thus remain consistent with the conclusions from a previous  $e^+\text{-Cd}$  scattering calculation [22].

The most likely source of error comes from the definition of the effective potential of the  $\text{Cd}^{2+}$  core. Our nonrelativistic model only includes relativistic effects indirectly, and it is possible that this leads to an overestimation of the Cd polarizability and thus the strength of  $e^+\text{-Cd}$  polarization potential. The uncertainty analysis reveals that the positron remains bound under a 10% reduction in the strength of the polarization interaction. However, the prominence of the  $p$ -wave resonance in the  $Z_{\text{eff}}$  spectrum is diminished, while the shoulder in the elastic cross section is not quite as obvious.

#### ACKNOWLEDGMENTS

This work was partially supported under the Australian Research Council's Discovery Program (Project No. 0665020). The computations were performed at the San Diego State University Computational Science Research Center, partially on facilities made available through the National Science Foundation (Grant CHE-0216563).

- 
- [1] J. Mitroy, M. W. J. Bromley, and G. G. Ryzhikh, *J. Phys. B* **35**, R81 (2002).
  - [2] M. W. J. Bromley and J. Mitroy, *J. Phys.: Conf. Ser.* **199**, 012011 (2010).
  - [3] C. M. Surko, G. F. Gribakin, and S. J. Buckman, *J. Phys. B* **38**, R57 (2005).
  - [4] G. G. Ryzhikh, J. Mitroy, and K. Varga, *J. Phys. B* **31**, 3965 (1998).
  - [5] J. Mitroy and M. W. J. Bromley, *Phys. Rev. Lett.* **98**, 173001 (2007).
  - [6] J. Mitroy, J. Y. Zhang, M. W. J. Bromley, and S. I. Young, *Phys. Rev. A* **78**, 012715 (2008).
  - [7] M. W. J. Bromley and J. Mitroy, *Phys. Rev. A* **73**, 032507 (2006).
  - [8] M. W. J. Bromley and J. Mitroy, *Phys. Rev. Lett.* **97**, 183402 (2006).
  - [9] J. P. Sullivan, S. J. Gilbert, S. J. Buckman, and C. M. Surko, *J. Phys. B* **34**, L467 (2001).
  - [10] S. J. Buckman and C. W. Clark, *Rev. Mod. Phys.* **66**, 539 (1994).
  - [11] M. W. J. Bromley and J. Mitroy, *Phys. Rev. A* **67**, 062709 (2003).
  - [12] M. W. J. Bromley and J. Mitroy, *Phys. Rev. A* **65**, 062505 (2002).
  - [13] J. Mitroy and M. W. J. Bromley, *Phys. Rev. A* **68**, 052714 (2003).
  - [14] S. G. Porsev and A. Derevianko, *JETP* **102**, 195 (2006).
  - [15] J. Mitroy, M. S. Safronova, and C. W. Clark, e-print arXiv:1004.3567 (2010).
  - [16] J. Y. Zhang, J. Mitroy, H. R. Sadeghpour, and M. W. J. Bromley, *Phys. Rev. A* **78**, 062710 (2008).
  - [17] D. Goebel, U. Hohm, and G. Maroulis, *Phys. Rev. A* **54**, 1973 (1996).
  - [18] D. Goebel and U. Hohm, *Phys. Rev. A* **52**, 3691 (1995).
  - [19] D. Goebel, U. Hohm, and K. Kerl, *J. Mol. Struct.* **349**, 253 (1995).
  - [20] A. Ye and G. Wang, *Phys. Rev. A* **78**, 014502 (2008).
  - [21] M. W. J. Bromley, J. Mitroy, and G. G. Ryzhikh, *Nucl. Instrum. Methods Phys. Res. B* **171**, 47 (2000).
  - [22] M. W. J. Bromley and J. Mitroy, *Phys. Rev. A* **65**, 062506 (2002).

- [23] A. W. Pangantiwar and R. Srivastava, *Phys. Rev. A* **40**, 2346 (1989).
- [24] S. N. Nahar, *Phys. Rev. A* **43**, 2223 (1991).
- [25] R. Szmytkowski, *Acta Phys. Pol. A* **84**, 1035 (1993).
- [26] V. A. Dzuba, V. V. Flambaum, G. F. Gribakin, and W. A. King, *Phys. Rev. A* **52**, 4541 (1995).
- [27] W. Müller, J. Flesch, and W. Meyer, *J. Chem. Phys.* **80**, 3297 (1984).
- [28] W. R. Johnson, D. Kolb, and K. Huang, *At. Data Nucl. Data Tables* **28**, 333 (1983).
- [29] Yu. Ralchenko, A. E. Kramida, J. Reader, and NIST ASD Team, *NIST Atomic Spectra Database* (version 3.1.5) (National Institute of Standards and Technology, Gaithersburg, MD, 2010), [<http://physics.nist.gov/asd3>].
- [30] C. E. Moore, *Atomic Energy Levels as Derived from the Analysis of Optical Spectra* (Molybdenum-Actinium NSRDS-NBS 35) (US Government Printing Office, Washington, DC, 1971), Vol. 3.
- [31] T. Andersen and G. Sorenson, *J. Quant. Spectrosc. Radiat. Transfer* **13**, 369 (1973).
- [32] A. Stathopoulos and C. Froese Fischer, *Comput. Phys. Commun.* **79**, 268 (1994).
- [33] J. Mitroy and G. G. Ryzhikh, *J. Phys. B* **32**, 2831 (1999).
- [34] J. Mitroy and M. W. J. Bromley, *Phys. Rev. A* **73**, 052712 (2006).
- [35] D. P. Carroll, H. J. Silverstone, and R. P. Metzger, *J. Chem. Phys.* **71**, 4142 (1979).
- [36] R. N. Hill, *J. Chem. Phys.* **83**, 1173 (1985).
- [37] M. W. J. Bromley and J. Mitroy, *Int. J. Quantum Chem.* **107**, 1150 (2007).
- [38] M. W. J. Bromley, J. Mitroy, and G. Ryzhikh, *J. Phys. B* **31**, 4449 (1998).
- [39] J. Mitroy and I. A. Ivanov, *Phys. Rev. A* **65**, 042705 (2002).
- [40] P. A. Fraser, *Adv. At. Mol. Phys.* **4**, 63 (1968).
- [41] R. P. McEachran, D. L. Morgan, A. G. Ryman, and A. D. Stauffer, *J. Phys. B* **10**, 663 (1977).
- [42] G. G. Ryzhikh and J. Mitroy, *J. Phys. B* **33**, 2229 (2000).
- [43] J. Mitroy and B. Barbiellini, *Phys. Rev. B* **65**, 235103 (2002).
- [44] J. Mitroy, *Phys. Rev. A* **72**, 062707 (2005).
- [45] E. Boronski and R. M. Nieminen, *Phys. Rev. B* **34**, 3820 (1986).
- [46] M. J. Puska and R. M. Nieminen, *Rev. Mod. Phys.* **66**, 841 (1994).
- [47] B. Barbiellini, in *New Directions in Antimatter Physics and Chemistry*, edited by C. M. Surko and F. A. Gianturco (Kluwer, Dordrecht, the Netherlands, 2001), p. 127.
- [48] M. W. J. Bromley and J. Mitroy, *Phys. Rev. A* **65**, 012505 (2001).